

A Climatology of the Circulation and Water Mass Distribution near the Philippine Coast*

TANGDONG QU AND HUMIO MITSUDERA

*Japan Marine Science and Technology Center, Yokosuka, Japan, and
International Pacific Research Center, SOEST, University of Hawaii, Honolulu*

TOSHIO YAMAGATA

Department of Earth and Planetary Physics, University of Tokyo, Tokyo, Japan

(Manuscript received 21 October 1997, in final form 27 July 1998)

ABSTRACT

This study provides a climatology of the circulation and water mass distribution by using historical data combined with observations from dozens of recent cruises near the Philippine coast. The most striking results are related to the poleward contraction of the subtropical gyre on denser surfaces, with the bifurcation of the North Equatorial Current moving from about 15°N in the upper thermocline to about 20°N at intermediate depths. Though time variability and the possible errors in the data are rather large, the Halmahera eddy (HE) is clearly seen in the climatic mean fields, lying at about 3°N, 130°E near the surface and reaching the Mindanao coast on density surfaces around $27.2\sigma_\theta$. It seems that the previously observed Mindanao Undercurrent is merely a component of the recirculation associated with the HE. North Pacific Tropical Water (NPTW) and Intermediate Water (NPIW) enter the western ocean with their extreme properties centered at 15° and 20°N, respectively, and continue southward as far as the southern tip of Mindanao along the western boundary. The influence of South Pacific sources becomes increasingly important with depth. Antarctic Intermediate Water (AAIW) is traced to about 12°N off Mindanao; but, there is little indication of a northward flow of AAIW farther north. Salinity extremes are also used as an indicator of NPTW and NPIW, and the primary result is that mixing of potential temperature and salinity are not jointly compensated, thus leading to an increase of density in NPTW and a decrease of density in NPIW in the flowpath from the North Pacific subtropical gyre to the Tropics along the Philippine coast.

1. Introduction

Recent studies of decadal climate variability have focused on the water mass exchange between the subtropical and equatorial oceans, particularly since the unusual climate state after 1990. There is increasing evidence that much of the water mass exchange between the subtropical and equatorial oceans occurs at the western boundary (Luyten et al. 1983; Lukas et al. 1991; Bingham and Lukas 1994; McCreary and Lu 1994; Lu and McCreary 1995). Here, a change in the properties of the subtropical surface waters will, in due course, first influence the equatorial thermocline and then the

surface conditions in the Tropics that in turn affect the circulation in the global atmosphere. The rapid atmospheric links between the Tropics and subtropics, and the slow oceanic links in the reverse direction are hypothesized to be essential in determining the decadal climate variability (Gu and Philander 1997). To further identify the mechanisms of decadal variability in the Pacific climate system, a comprehensive study of the circulation and water mass distribution in the tropical western Pacific is of high scientific interest.

Studies of the tropical western Pacific have been fairly diverse (cf. Fine et al. 1994); in general, they can be divided into two groups. One includes the early work of Reid (1965), Tsuchiya (1968), and many others, who investigated the large-scale aspects of water masses by using data collected from various cruises in different seasons. These studies were useful because they provided the basis for understanding the water characteristics of the entire tropical Pacific Ocean. However, owing to the sparse distribution of the data used, these studies failed to depict many detailed phenomena associated with the narrow western boundary currents. A

*School of Ocean and Earth Science and Technology Contribution Number 4769.

Corresponding author address: Dr. Tangdong Qu, International Pacific Research Center, SOEST, University of Hawaii, 2525 Correa Rd., Honolulu, HI 96822.
E-mail: tangdong@soest.hawaii.edu

relatively good data coverage is available for the tropical western Pacific since the 1970s, particularly after the success of the Tropical Ocean Global Atmosphere (TOGA) and the World Ocean Circulation Experiment (WOCE) programs, and, consequently, many alternative studies, that can be put under the second group, have appeared. Among them, Toole et al. (1988), Wijffels et al. (1995), and Qu et al. (1997, 1998) focused on the mean structure along repeated sections, whereas Tsuchiya et al. (1989), Lukas et al. (1991), Fine et al. (1994), Bingham and Lukas (1994, 1995), and many others examined the synoptic distribution over a large part of the tropical western Pacific. These studies have substantially advanced our knowledge of the western boundary currents and their potentially important role in the water mass exchange between the subtropical and equatorial oceans. However, the results may have some limitations because measurements with extensive coverage both in space and time were not used. At this stage, it seems desirable to prepare a climatology of the circulation and water mass distribution over the entire tropical western Pacific with all available data.

Huge historical data were distributed recently by NOAA/NESDIS/NODC (called the NODC data below). The NODC data, augmented by observations from dozens of recent cruises, likely provide the best data coverage to date in the tropical western Pacific, thus allowing a more accurate and more general investigation of the region, in particular with regard to the intermediate waters. The results of an analysis of these data are presented in the following sections. After a brief description of the data in section 2, general characteristics of water masses are presented in section 3. Sections 4 and 5 are devoted to detailed descriptions of water properties on isopycnal surfaces and on vertical sections, respectively. Error analysis is made in section 6. An attempt is also made in section 7 to trace the North Pacific waters by property extremes. Results are summarized in section 8.

2. Description of data

For this study CTD and bottle profiles at observed levels recorded on the CD-ROMs of *World Ocean Atlas 1994* of NOAA/NESDIS/NODC from the region 2°S – 27°N , 118° – 142°E were used. The observed level profiles were used instead of the mean atlases at standard depths for a couple of reasons. First, the objective analysis employed in preparing the mean atlases involves horizontal smoothing over approximately 1000 km, and thus the smoothed fields may not be appropriate for showing some of the detailed phenomena at the western boundary. Second, averaging at standard pressure surfaces may produce drastic artificial smoothing of water properties due to the huge vertical gradient around the pycnocline.

Also included in this study were data from 23 recent hydrographic cruises under the auspices of TOGA and WOCE, including five by the Chinese Academy of Sci-

ences (CAS; Qu et al. 1998), eight by a joint program between the People's Republic of China and the United States (PRC-US; Toole et al. 1990), one by the Western Equatorial Pacific Ocean Circulation Study program (WEPOCS III; Lukas et al. 1991), two by a joint program between Japan Marine Science and Technology Center and Badan Pengkajian Dan Penerapan Technology of Indonesia (JAMSTEC-BPPT; Kashino et al. 1996), and six obtained from the WOCE Hydrographic Program Special Analysis Center. It is worthwhile noting that the CTD profiles from the first eight PRC-US cruises and the WEPOCS III have already been included in the NODC archives. However, for unclear reasons, the record was made only for approximately the upper 400 m. For this study these shallower profiles were replaced by the high-resolution data cited above.

Even after extensive editing (Levitus and Boyer 1994a–c), some NODC profiles still contained erroneous records both in coordinates and measured values. The primary procedure for quality control of the data for this study included removal of profiles with obviously erroneous records (e.g., temperature higher than 8°C below 1000 m or salinity lower than 30 psu below 100 m) and profiles with only a few measurements in the shallow (<100 m) waters and at deep (>700 m) levels as well, without any in between. The most difficult quality control process involved the oxygen profiles since different units were used, with some in ml l^{-1} and some in $\mu\text{mol kg}^{-1}$. These were detected by eye. After all these procedures, the historical and recent data consisted of 14 540 temperature/salinity and 6193 oxygen profiles for the region studied (Figs. 1a and 1b). The observations of temperature/salinity spanned the period from the 1920s to the beginning of the 1990s, with two periods of dense sampling during 1935–45 and 1965–90, respectively (Fig. 2). Oxygen measurements were not wide spread until the 1960s. No obvious bias in the density of sampling was apparent toward any season of the year.

3. General characteristics

The relations of potential temperature versus salinity and dissolved oxygen concentration versus salinity are shown on a $5^{\circ} \times 5^{\circ}$ grid for all observed level readings (Figs. 3a,b). At least five water masses are indicated in these relations. One is in the surface layer, two are in the upper thermocline, and two are in the intermediate layers. The tropical surface water (TSW), with a homogeneous layer of oxygen concentration (4.5 ml l^{-1}) at $25^{\circ} < \theta < 30^{\circ}\text{C}$ and $33.5 < S < 34.5$ psu, is formed locally in the vicinity of the intertropical convergence zone (ITCZ). It is confined primarily south of 15°N in the ocean interior, but may be traced farther north at the western boundary.

North Pacific Tropical Water (NPTW) is characterized by high salinity ($34.75 < S < 35.25$) and high oxygen concentration ($>4.0 \text{ ml l}^{-1}$) on density surfaces around

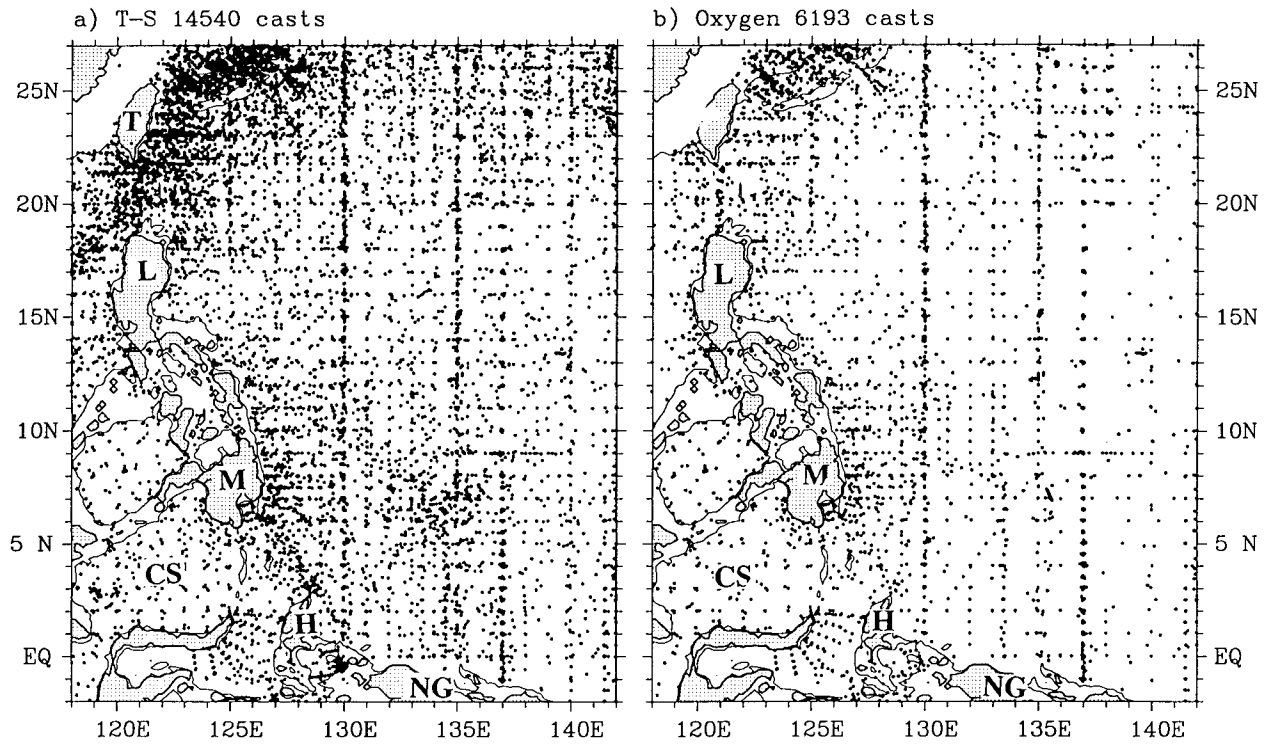


FIG. 1. Spatial distribution of stations (asterisk) of (a) temperature/salinity and (b) oxygen for this study. The light line shows the 500-m isobath. Abbreviations are CS: Celebes Sea, H: Halmahera, L: Luzon, M: Mindanao, NG: New Guinea, and T: Taiwan.

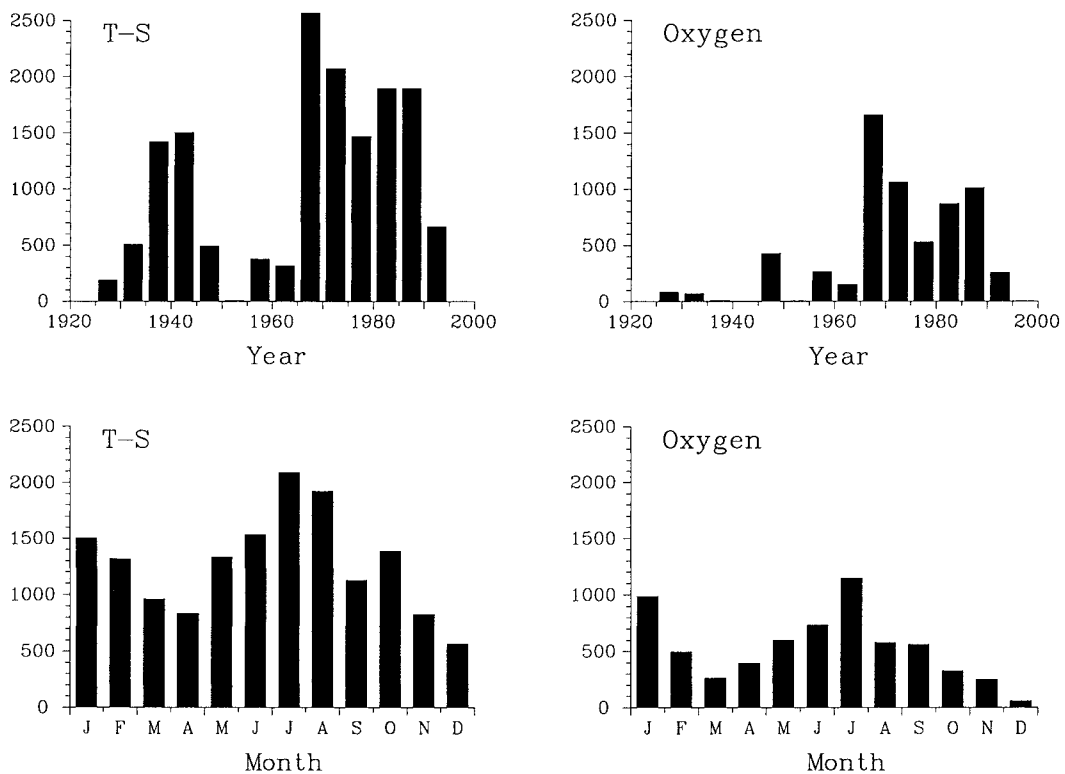


FIG. 2. Temporal distribution of stations for this study.

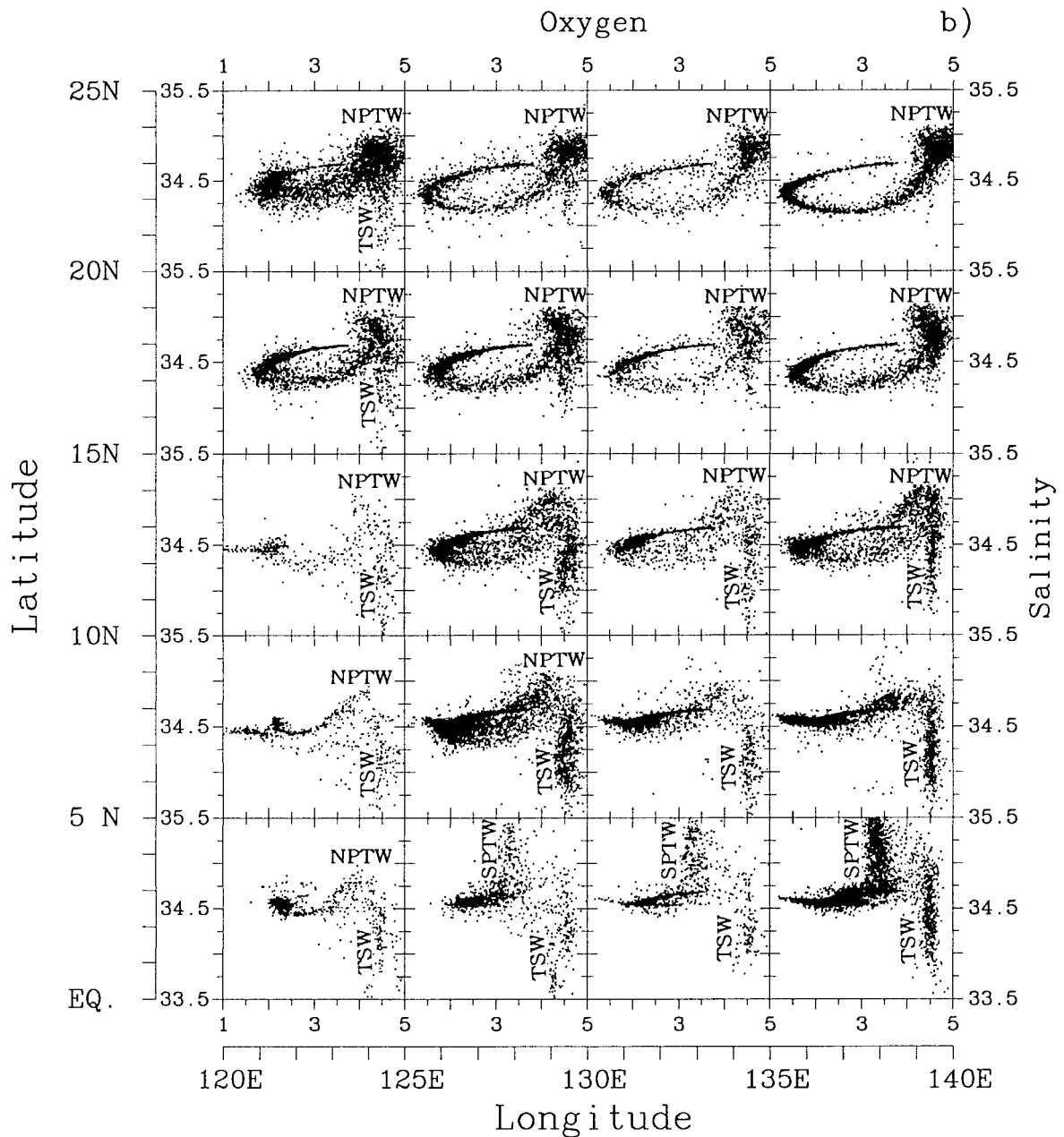


FIG. 3. (Continued.)

This water appears to cross much of the interior ocean within the subtropical gyre, with only a small part escaping to the Tropics at the Philippine coast. Below the NPIW salinity minimum, oxygen concentrations tend to decrease with depth, reaching the broad minimum (<2.0 ml l^{-1}) of the North Pacific subpolar water (Reid 1965; Wijffels et al. 1998). The difference in depth between the salinity and oxygen minima induces circle-shaped $S-O_2$ relations (Fig. 3b) in the north. These relations are not seen south of $10^\circ N$, presumably because of the intrusion of South Pacific waters with relatively high

oxygen levels. A secondary salinity minimum (about 34.55 psu) characteristic of Antarctic Intermediate Water (AAIW; Wyrki 1961) is present near the equator around the $27.2\sigma_\theta$ surface (Fig. 3a).

4. Mean distributions on isopycnal surfaces

Maps are presented to show the distributions of acceleration potential, depth, salinity, and oxygen concentration on three isopycnal surfaces. The geostrophic flow along isopycnal surfaces can be deduced from the

gradient of the acceleration potential (Tsuchiya 1968). Water properties are conserved following isopycnal flow, assuming the flow is inviscid and nondiffusive. In the presence of viscosity and diffusivity, as is the case in the true ocean (sections 4a–c), the flow does not have to be exactly along constant property lines. Nevertheless, water properties (temperature, salinity, oxygen concentration, etc.) can be used as passive tracers to provide direct pathways of water masses. Because temperature on isopycnal surfaces is uniquely defined by salinity, maps of temperature resemble those of salinity in all the details, and are excluded from this study.

The three isopycnal surfaces chosen are $\sigma_\theta = 24.5$, 26.6, and 27.2 (Fig. 3a). They have the following characteristics. The $24.5\sigma_\theta$ surface passes through the upper thermocline at depths of 100–200 m, lying roughly between NPTW and SPTW. The choice of the $26.6\sigma_\theta$ surface is based on the fact that NPIW is of lower (about $26.55\sigma_\theta$) density at the Mindanao coast (Lukas et al. 1991) than in the main part of the subtropical gyre ($26.8\sigma_\theta$, Talley 1993). Thus, this surface is expected to have a more reasonable representation of NPIW than the $26.8\sigma_\theta$ surface for much of the region studied. The $27.2\sigma_\theta$ surface coincides basically with the secondary vertical salinity minimum (AAIW) that spreads over the southern part of the Philippine Sea.

While deeper observations are available at some locations and times, the number of observations decreases rather rapidly with depth below 1200 db. To optimize uniformity of the database, the reference level for estimating acceleration potential is chosen to be 1200 db. Because of the shallowness of the three isopycnal surfaces chosen, whose depths do not exceed 900 db over the whole region studied, this reference is thought to be deep enough to show most major features of the geostrophic flow in the upper layers.

Water properties at observed levels are first interpolated onto the selected isopycnal surfaces by cubic spline, and then averaged on a $0.5^\circ \times 0.5^\circ$ grid, regardless of their date and time of measurement. Considering that there are few stations in some grid bins, we smooth the property fields by choosing a horizontal radius big enough to include at least 20 observations in each grid bin from which means and standard deviations were calculated. The primary criterion for averaging is that two widely spaced data points have more influence on the mean than two close together. Estimates of standard deviations are used to edit the mean: if an interpolated property deviates from the mean by a value three times larger than the standard deviation, it is excluded, and the mean and standard deviation are recalculated. The estimated mean fields are finally smoothed with a Gaussian filter of about 150-km half-width or e -folding scale (Bretherton et al. 1976).

a. $\sigma_\theta = 24.5$

The geostrophic flow on the $24.5\sigma_\theta$ surface shows many similar features to those derived from synoptic

observations (e.g., Nitani 1972; Lukas et al. 1991). The westward-directed NEC is seen over a broad latitude range between 8° and 25°N . It splits near 15°N at the western boundary into the northward-flowing Kuroshio and southward-flowing MC (Fig. 4a). The boundary between the NEC and the North Equatorial Countercurrent (NECC) is clearly indicated by a minimum ($<15.5 \text{ m}^2 \text{ s}^{-2}$) of acceleration potential at about 7°N . Part of the MC appears to turn cyclonically in the Celebes Sea to feed the NECC, adding to waters that flow directly from the MC to the NECC. The retroflection of the MC in the Celebes Sea and its subsequent flow to the east generates a trough ($<130 \text{ m}$) in the isopycnal surface centered at 7°N , 129°E (Fig. 4b), consonant with the previously observed Mindanao eddy (Wyrki 1961; Lukas et al. 1991). A small anticyclonic eddy (acceleration potential $>16.5 \text{ m}^2 \text{ s}^{-2}$) near 3°N , 130°E may represent the Halmahera eddy, through which the South Equatorial Current tends to recurve into the NECC.

The deepest ($>180 \text{ m}$) isopycnal depth lies farther south (15°N) than the northern boundary of the NEC, consonant with the poleward contraction of the subtropical gyre with depth (Reid and Arthur 1975). As the northward downslope of isopycnal surfaces corresponding to the westward NEC extends farther north in the deeper layers, there should be a northward displacement of the maximum of acceleration potential from that of depth (ridge) on the shallower surfaces. From this ridge isopycnal depth decreases northward to about 110 m near 25°N , reflecting the dominant influence of latitude-dependent surface heat flux on the upper thermocline water.

High salinity water originating in the tropical surface salinity maximum of the North Pacific (NPTW) is seen as a tongue with salinity exceeding 34.95 psu (Fig. 4c). The axis of the tongue appears to coincide with the ridge of the isopycnal surface and with the bifurcation of the NEC as well. It is likely that this high salinity water flows westward in the NEC and reaches the Philippine Islands in a latitude band centered near 15°N , where part of it returns northward in the Kuroshio and the rest continues southward in the MC.

High oxygen levels extending from the NEC southward along the Philippines and toward the Makassar Strait reflect the strong influence of North Pacific sources on the water masses in the Celebes Sea (Fig. 4d). High oxygen levels also extend southeastward off Mindanao, indicative of a direct advection of NPTW to the NECC. The alternating tongues of high and low oxygen level between 5° and 7°N farther to the east might be related to the meandering of the NECC. A strong meridional temperature and salinity gradient, allied with homogeneous oxygen concentration, is seen east of Halmahera, which has been interpreted as evidence that South Pacific waters do not directly cross the equator in the interior ocean but retroflect into the equatorial currents as they arrive at the equatorial western Pacific (Fig. 4a; Tsuchiya et al. 1989; Fine et al. 1994).

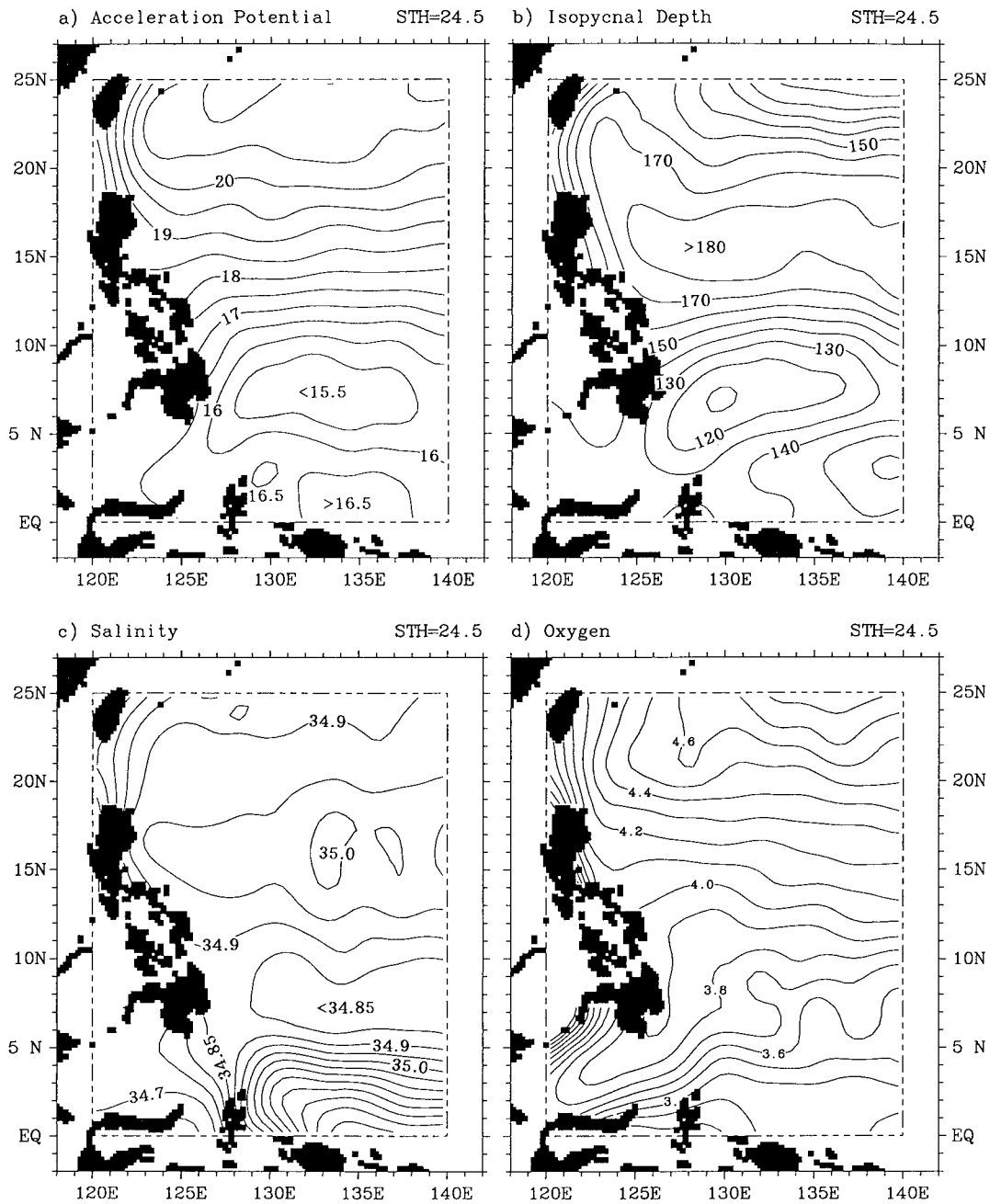


FIG. 4. Distributions of (a) acceleration potential (in $\text{m}^2 \text{s}^{-2}$) relative to 1200 db, (b) isopycnal depth in meter, (c) salinity (in psu), and (d) dissolved oxygen concentration (in ml L^{-1}) on $24.5\sigma_\theta$ surface.

b. $\sigma_\theta = 26.6$

The NEC on the $26.6\sigma_\theta$ surface (Fig. 5a) shows essentially the same pattern as that in the upper thermocline except for a slight northward shift (to about 17°N) of the bifurcation latitude. A striking feature of the isopycnal topography is that the ridge measured at about 15°N in the shallower water (Fig. 4b) does not exist on the $26.6\sigma_\theta$ surface; instead, the isopycnal depth appears

to increase northward from about 275 m near 7°N to about 600 m near 25°N . This result implies that the latitude-dependent surface heat flux has little impact on the waters of the salinity minimum. Eastward-directed subsurface flow is seen from about 5°N to near the equator; its southern boundary is not particularly well defined, presumably due to the emergence of the Equatorial Undercurrent. Another important feature of geo-

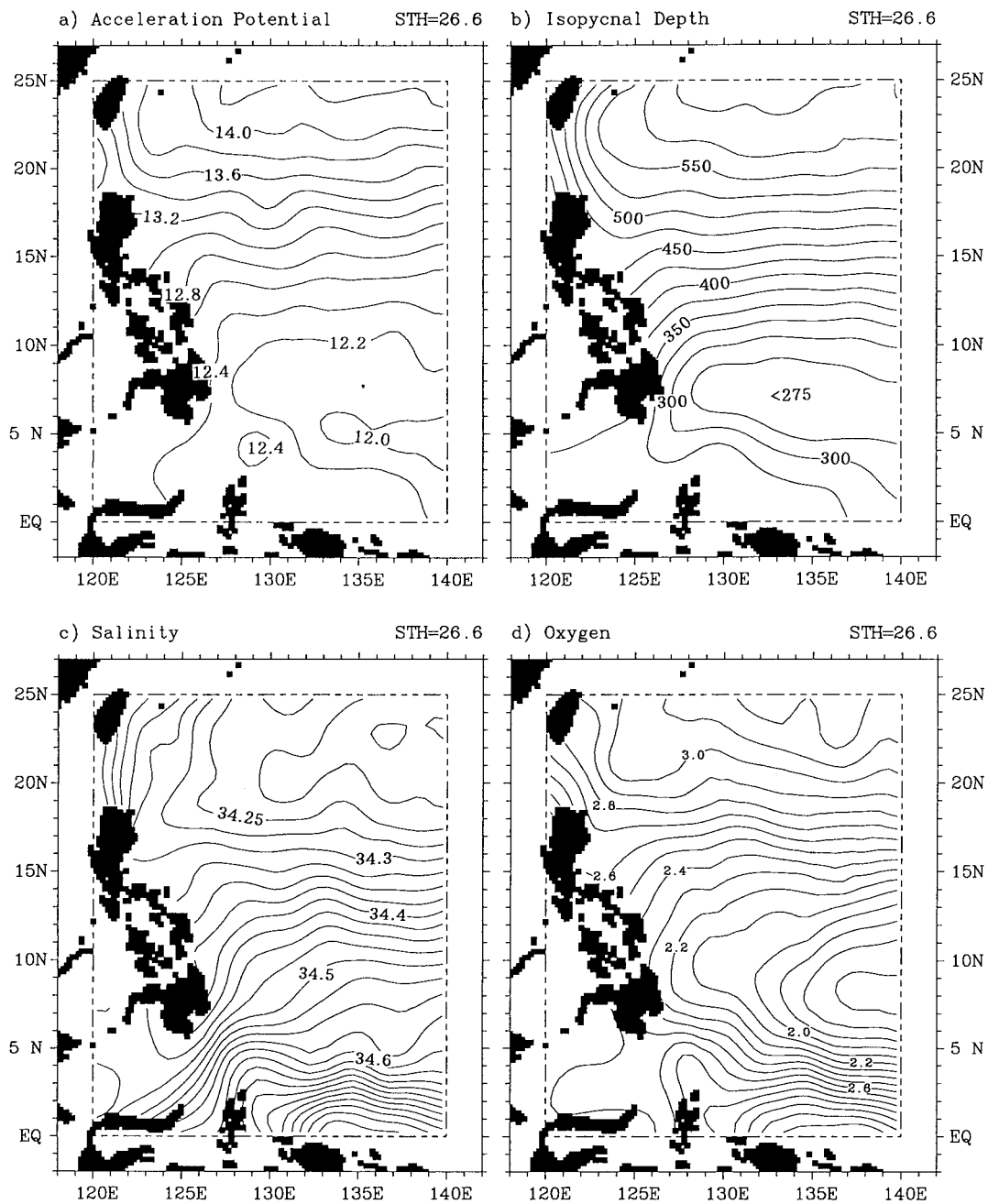


FIG. 5. Same as Fig. 4 except on the $26.6\sigma_t$ surface.

strophic flow is that the Halmahera eddy, indicated as a maximum ($>12.4 \text{ m}^2 \text{ s}^{-2}$) of acceleration potential, appears to move somewhat farther northwest than on the shallower surface (Fig. 4a).

Low salinity water characteristic of NPIW is seen as a tongue extending southwestward in the NEC and southward in the Luzon Undercurrent (LUC; Qu et al. 1997) and the MC along the Philippine coast (Fig. 5c). The salinity in the tongue is lowest (about 34.0 psu) in the northeast, and increases to about 34.4 psu around

the southern tip of Mindanao by lateral mixing with more saline waters of its surroundings. Associated with this low salinity tongue is an elevated oxygen level that decreases southward from the NEC and eastward from the LUC/MC (Fig. 5d). A boundary between water masses is found east of Mindanao. Bingham and Lukas (1994) describe this boundary as a water mass discontinuity between the equatorial and subtropical waters. The equatorial water is seen extending westward as a tongue of low ($<2.0 \text{ ml l}^{-1}$) oxygen concentration cen-

tered at about 8°N. On the inshore side, water of North Pacific origin (NPIW) escapes to the equatorial region via the MC. Compared to the shallower surface, water originating from the Southern Hemisphere with high salinity and high oxygen concentration intrudes farther northwest, consonant with the northwestward shift of the Halmahera eddy on this surface (Fig. 5a).

c. $\sigma_\theta = 27.2$

The NEC on the $27.2\sigma_\theta$ surface shrinks northward north of 15°N, with its bifurcation occurring near 20°N. This implies that the LUC, though significantly reduced in magnitude from the surfaces above, originates as far north as 20°N on this surface. The LUC at this density does not appear to go directly southward along the western boundary but separates from the coast around 10°N. Probably, this flow turns to the right continuously and finally reaches the equatorial region through a clockwise recirculation east of Mindanao.

The distribution of isopycnal depth (Fig. 6b) basically fits the geostrophic flow. A minimum (<700 m) of isopycnal depth is located near 12°N, somewhat farther south than the minimum (<9.65 m² s⁻²) of acceleration potential due to the same reason as was stated in section 4a. A maximum of isopycnal depth (>750 m) is found east of Mindanao, coinciding roughly with the maximum (>9.75 m² s⁻²) of acceleration potential.

The recirculation regime east of Mindanao was not previously reported, though it could be sometimes identified from one- or two-shot hydrographic observations (e.g., Kashino et al. 1996, their Fig. 10c). To detect it, several density surfaces between 26.7 and $27.4\sigma_\theta$ were examined. In all of these maps (not shown) a core of high acceleration potential with deep isopycnal depth is present. The location varies with density from about 4°N on $\sigma_\theta = 26.6$ to about 7°N on $\sigma_\theta = 27.0$. This pattern (Figs. 6a,b) appears to remain in denser waters ($27.0 \leq \sigma_\theta \leq 27.4$), despite some quantitative modifications. Furthermore, Figs. 6a,b are insensitive to vertical displacements of the reference level within the depth range of 1000–1500 db. All these results suggest that the recirculation regime east of Mindanao is a robust feature.

Water of subpolar origin (Reid 1965; Wijffels et al. 1998) with $S < 34.4$ psu is seen extending westward in the NEC and southward in the LUC (Fig. 6c). Water with relatively homogeneous salinity (about 34.55 psu) and high (>2.0 ml l⁻¹) oxygen concentration identical with the properties of AAIW meets North Pacific water in a broad region between Halmahera and Mindanao. Much of the AAIW appears to be advected eastward into the equatorial circulation, with a part escaping to the Celebes Sea. The northward intrusion of AAIW is traced to about 12°N at the Mindanao coast, in reasonable agreement with the early work of Masuzawa (1972).

The previously observed Mindanao Undercurrent (MUC; Hu et al. 1991; Lukas et al. 1991) appears to

be merely a component of recirculation associated with the Halmahera eddy. Using 10 repeated hydrographic sections along 8°N east of Mindanao, Qu et al. (1998) noted that the MUC, referred to as subsurface northward velocity cores centered at 800–900 db, was evident during all the periods of observation, having mean speed exceeding 0.08 m s⁻¹. The geostrophic flow shown in Fig. 6a appears to match their results very well, supporting the speculation that the MUC is a permanent feature. Water joining the Halmahera eddy from the south may be advected northward via the MUC along the coast of Mindanao and carried offshore on the north side of the gyre, where it either continues as a jet into the equatorial currents or turns southward to complete the circuit. Recirculation east of Mindanao allows water particles to gradually share properties with their surroundings and finally approach a common and homogenized state. This probably explains why mean property distribution does not show any significant cores in the narrow MUC except for a broad region of elevated oxygen level east of Mindanao (Fig. 6d; Wijffels et al. 1995; Qu et al. 1998).

Here, we emphasize the potentially important influence of eddies through integration over short timescales on the distribution of properties, for example, the concentration of dissolved oxygen (Fig. 6d). According to several earlier studies (e.g., Masumoto and Yamagata 1991; Qiu and Lukas 1996), the tropical western Pacific is an eddy-dominated region. With the growth and decay of the Halmahera eddy, water that flows to the north is usually of higher oxygen level than that to the south in the front area between the North and South Pacific waters (Fig. 6d). The overall action of eddies would be to produce a net (northwestward) transport of oxygen in the downstream direction of the MUC, but its relative importance to the mean advection is not clear.

5. Mean distributions along vertical sections

Maps of salinity and oxygen concentration are shown against density along two meridional and eight zonal sections. The meridional sections are chosen to be two regularly repeated hydrographic sections at 130° and 137°E with usually 30–60 samples in each 1° lat bin. The selection of zonal sections is made at every 2° lat from 6° to 20°N at the western boundary (west of 130°E). Sampling along the zonal sections is generally good on a 1° lat × 0.5° long grid, except at 14° and 16°N where broader (1.5° instead of 1°) latitude bands are chosen so as to include at least five samples within each 0.5° long bin. Mean sections are constructed by ensemble averaging.

a. Meridional

Along 137°E, NPTW is indicated by a high salinity (>34.90 psu) core stretching from about 10° to 24°N on density surfaces between 23.0 and $25.0\sigma_\theta$ (Figs.

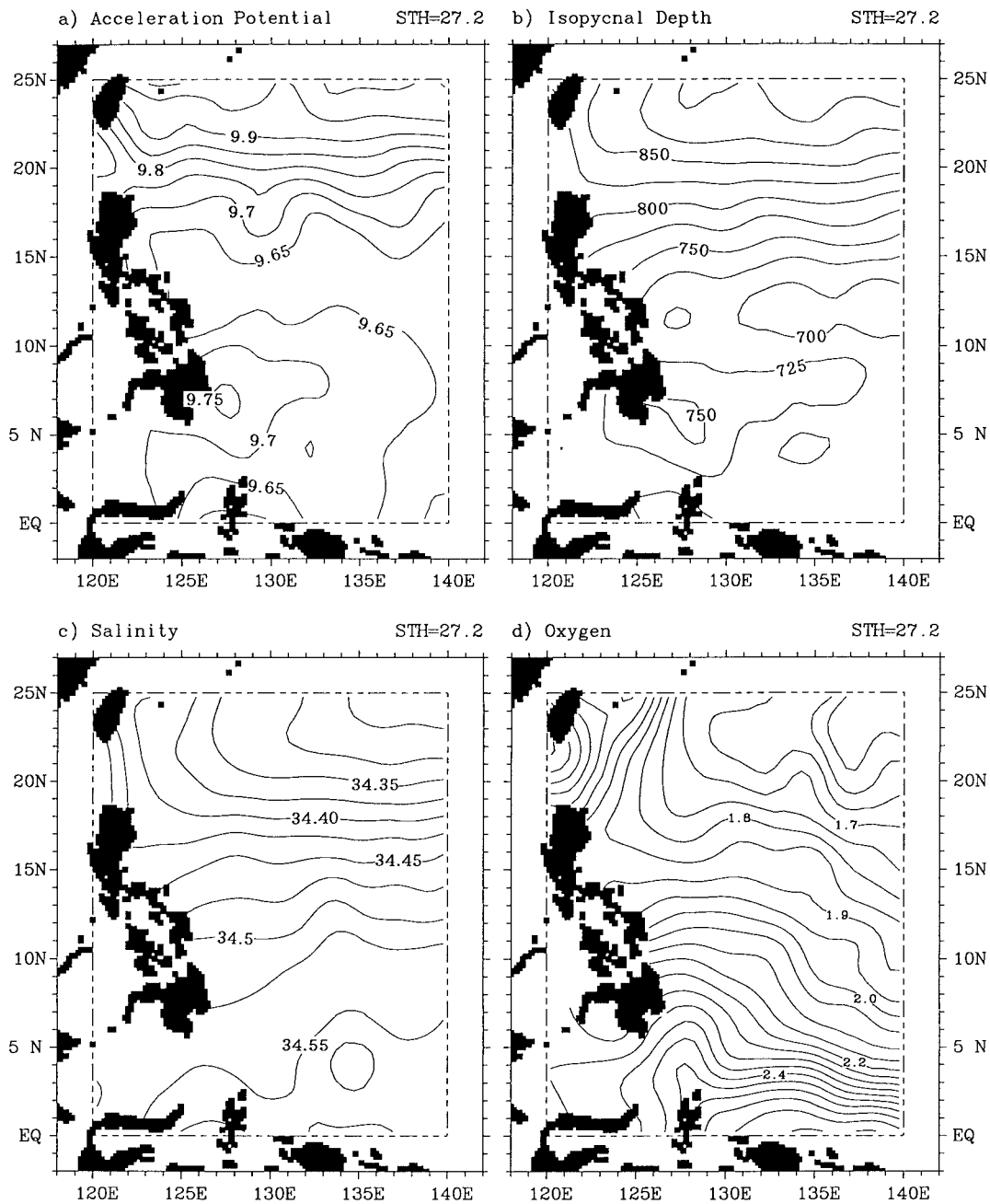


FIG. 6. Same as Fig. 4 except on the $27.2\sigma_\theta$ surface.

7a,b). The highest (>35.05 psu) salinity of NPTW is found near 15°N around $\sigma_\theta = 24.0$. Below NPTW, salinity decreases with depth and reaches a minimum (<34.20 psu) at about $26.8\sigma_\theta$ (NPIW), with a slight decrease in density toward the south. NPIW salinity is lowest (<34.2 psu) at 20° – 25°N and is less than 34.40 psu in a broad band north of 13°N .

Oxygen concentration along the section shows a pattern consistent with that discussed for salinity. NPIW resides on a strong vertical gradient of oxygen (Fig. 7b),

marking the bottom of recently ventilated thermocline water (Qiu 1995). Below NPIW is a broad minimum of oxygen (<2 ml l^{-1}) stretching southward from the northern end of the section. The oxygen minimum is confined on density surfaces around $27.3\sigma_\theta$ in the subtropical region, but is seen near $26.8\sigma_\theta$ at 5°N . The shoaling of this oxygen minimum could be due to the northward intrusion of AAIW. Indeed, water with a typical salinity minimum (about 34.55 psu) of AAIW and elevated oxygen level is found below the oxygen min-

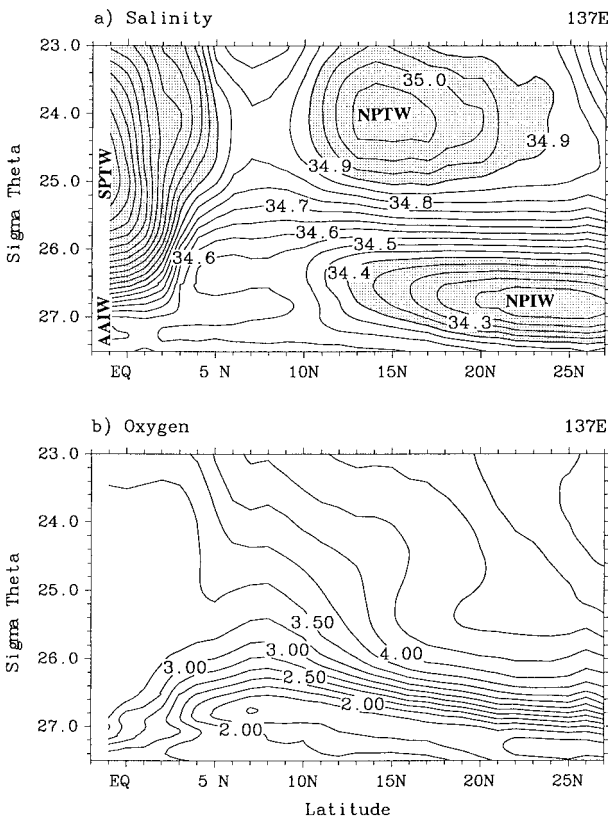


FIG. 7. Vertical sections of (a) salinity (in psu) and (b) dissolved oxygen concentration (in ml L^{-1}) against σ_θ along 137°E . The areas with $S > 34.9$ psu or $S < 34.4$ psu are shaded.

imum in the Tropics. SPTW, corresponding to high salinity (>34.9 psu) and homogeneous oxygen concentration (about 3.5 ml l^{-1}), forms a very thick layer between 23.0 and $26.5\sigma_\theta$ surfaces, with extreme properties at about $25.0\sigma_\theta$.

The extreme properties of NPTW and NPIW become weaker toward the west due to the mixing in the ocean. Along 130°E , the spreading of NPTW is between 10° and 20°N , with its highest salinity (>35.0 psu) at about 15°N . NPIW salinity is lowest (<34.20 psu) near 20°N and is less than 34.40 psu along the northern part of the section (Fig. 8a). The southern boundary of the oxygen minimum ($<2.0 \text{ ml l}^{-1}$) is seen at about 7°N , somewhat farther north than that along 137°E , reflecting the strong influence of South Pacific sources on the water masses near the western boundary.

b. Zonal

NPIW enters the western ocean as part of the NEC centered near 20°N (Fig. 9a), and extends southward along the Philippine coast (Figs. 9b–h). At 16°N , it contains two cores of low salinity (<34.30 psu). One hugs the coast and can be traced continuously to as far as the southern tip of Mindanao; while the other, emanating

from the east, is not present south of 14°N , reflecting the limited extension of NPIW in the ocean interior (Fig. 8a). The low salinity cores along the coast have relatively high oxygen levels, consonant with its supply from the subtropical gyre. This is clearly indicated by the shoreward downslope of oxygen concentration contours south of 16°N .

NPTW reaches the Philippine coast with its extreme properties ($S > 35.0$ psu) at 14° – 16°N (Figs. 9c–d) where it separates into two parts. One turns northward into the East China Sea via the Kuroshio (Figs. 9a–b), and the other moves southward in the MC (Figs. 9e–h). As NPTW approaches the Mindanao coast, its salinity maximum hugs the continental slope with a value about 0.10 psu lower than at the bifurcation latitude of the NEC because of mixing. In the ocean interior, the spreading of NPTW is seen as a high salinity core stretching from the east near the bifurcation latitude of the NEC (Figs. 9b–e), but this structure is absent farther north and south. Because of its subtropical origin, NPTW supplied by the MC is of elevated oxygen level south of 14°N (Figs. 9e–h). This condition is reversed north of 16°N , with relatively low oxygen concentration in the Kuroshio (Figs. 9a and 9b).

6. Error analysis

As stated in section 2, the observations used in this study were made in various seasons of different years. Since the tropical western Pacific is a region of strong eddies, in particular those associated with transeasonal and/or interseasonal fluctuations, time variations in the region are expected to be fairly large (e.g., Lukas et al. 1991; Masumoto and Yamagata 1991; Qiu and Lukas 1996). Indeed, this is confirmed by large standard deviations of properties obtained during the averaging and smoothing processes.

The spatial distribution of standard deviations, though not presented here, is rather uniform on the three isopycnal surfaces, except with slightly higher values in the front area between the North and South Pacific waters east of Halmahera. Typical temperature and salinity standard deviations, defined as the averages over the domain, are 0.32°C and 0.10 psu on $\sigma_\theta = 24.5$, 0.35°C and 0.07 psu on $\sigma_\theta = 26.6$, and 0.24°C and 0.04 psu on $\sigma_\theta = 27.2$, based on ensembles of more than 20 stations in each $0.5^\circ \times 0.5^\circ$ bin. Consequently, acceleration potential (as a vertical integration of steric anomaly) varies considerably, with typical standard deviations of 0.72 , 0.33 , and $0.15 \text{ m}^2 \text{ s}^{-2}$, respectively, on the three surfaces. The standard deviation of the depth of the $27.2\sigma_\theta$ surface (52 m) is about two times larger than that of the $24.5\sigma_\theta$ surface (25 m), indicative of larger uncertainties in the deeper layers. Estimate of the standard deviations of oxygen concentration of 0.25 , 0.26 , and 0.16 ml l^{-1} on the three surfaces provides independent information on the variability. Standard deviations of properties are also obtained along vertical

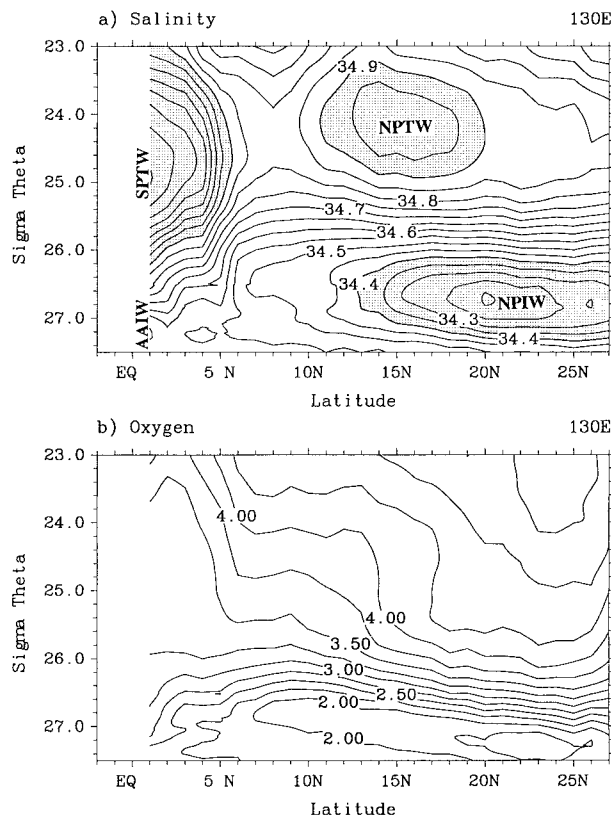


FIG. 8. Same as Fig. 7 except along 130°E.

sections, showing a pattern consistent with that on the isopycnal surfaces; but, the magnitude is somewhat smaller because of the relatively good data coverage along the selected vertical sections (section 5).

The results described above give the impression that the standard deviations of properties are of comparable strength with the mean fields, in particular with regard to the waters of the salinity minimum. However, it must be noted that, in addition to time variations, the estimated standard deviations may also include uncertainties in the data mainly from the following three sources. First, because most of the observations were made at conventional standard depths, the interpolated values of properties on the isopycnal surfaces are subject to a large uncertainty, in particular at the intermediate depths where vertical separation between levels is typically 100 m. Second, the limited number of observations may enhance the uncertainty by using a larger radius of averaging in some parts of the region. The third and probably the least important source of the uncertainty is due to the smoothing process, explaining less than 10% of the total standard deviations.

Yet there is no easy way to definitely know how much of the large standard deviation is due to the errors in the data, so as to quantify how complete the mean fields (Figs. 4–9) are in a statistical sense. Nevertheless, since

both time variability and the effect of the errors in the data are expected to be much reduced by the combined use of more than 20 samples from various cruises in different seasons of different years, the mean fields described in the preceding sections should be reasonably representative.

7. Salinity extremes as an indicator of water masses

Water masses have been traced using isopycnal surfaces in the previous sections, based on the idea that water flows adiabatically without mixing. But, in the presence of mixing, as is the case in the real ocean, can mixing of temperature and salinity be jointly compensated for a water mass to remain a stable density? This question is investigated below by using salinity extremes as an indicator of water masses.

a. NPTW

Based on Figs. 7–9, NPTW is traced as a salinity maximum (>34.85) in the density range of 23.0–25.0 σ_θ . Where multiple maxima occur, the one of highest salinity is used to map NPTW properties (Figs. 10a–d). In the distribution of the probability of salinity maximum within the density range cited above (Fig. 10a), the location of NPTW is fairly clear. Probability higher than 0.5 fits the isopycnal distributions (Figs. 4a–d) fairly well. It is confined primarily north of 10°N in the ocean interior, but extends farther south along the western boundary. Another interesting phenomenon shown in Fig. 10a is a belt of high (>0.8) probability stretching westward over the latitude range between 12° and 18°N. The axis of the belt is consistent with the preceding description (section 4) that NPTW enters the western ocean with extreme properties at about 15°N. Relatively high probability extending northwestward along the coast of New Guinea is also seen, apparently due to the intrusion of SPTW.

The density of NPTW alters between 23.9 and 24.4 σ_θ over the domain enclosed by the probability higher than 0.5 (Fig. 10b). It is lowest (23.9 σ_θ) near 15°N, 140°E, and increases westward in the NEC, northward in the Kuroshio, and southward in the MC, achieving 24.25 and 24.10 σ_θ , respectively, at the northern and southern tips of the Philippines. In the meantime, considerable changes are found in potential temperature and salinity, both decreasing in the downstream direction of the NEC, the Kuroshio, and the MC (Figs. 10c–d). The reason for these changes are apparently mixing in the ocean.

Here σ_θ is a function of potential temperature, salinity, and pressure of seawater. Different variables make different contributions. The component of pressure is generally negligible in the upper ocean, so the density of water masses is basically determined by the relative importance of potential temperature and salinity in the state equation. In the limit of linear thermodynamics,

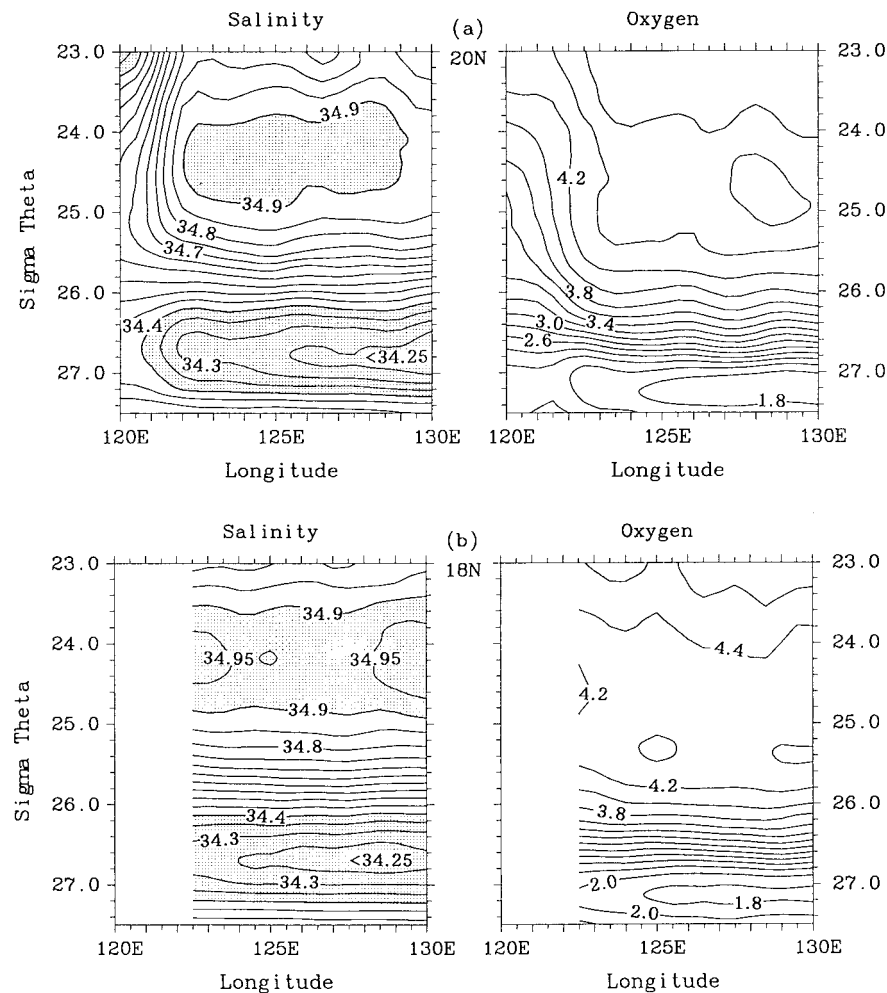


FIG. 9. Vertical sections of salinity in psu and dissolved oxygen concentration (in ml L^{-1}) against σ_θ along (a) 20°N , (b) 18°N , (c) 16°N , (d) 14°N , (e) 12°N , (f) 10°N , (g) 8°N , and (h) 6°N . The areas with $S > 34.9$ psu or $S < 34.4$ psu are shaded.

changes in density due to changes in potential temperature can be estimated by assuming a constant salinity, and vice versa. With the properties shown in Figs. 10c–d, the increase of density due to the decrease of potential temperature is about three and a half times larger in magnitude than the decrease of density due to the decrease of salinity, thus making NPTW gain its density gradually as it flows with the NEC, the Kuroshio, and the MC.

b. NPIW

NPIW properties have been documented by several earlier studies as a salinity minimum between 26.6 and $27.0\sigma_\theta$ (e.g., Reid 1965; Talley 1993). Considering that NPIW is of lower (about $26.55\sigma_\theta$) density at the Mindanao coast (Lukas et al. 1991), a wider density range of 26.4 – $27.0\sigma_\theta$ is chosen here in which to search for NPIW. The distribution of high (>0.5) probability (Fig.

11a) of salinity minimum (<34.45 psu) in this density range shows a similar pattern to that of salinity maximum (Fig. 10a), except for a northward shift of the southern boundary in the ocean interior due to the contraction of the subtropical gyre on denser surfaces. The highest (>0.8) probability is centered near 20°N , coinciding roughly with a cold and fresh water mass characteristic of NPIW.

NPIW properties are significantly modified as a result of mixing, becoming warmer and saltier in the downstream direction of the flowpath (Figs. 11c–d). Again, because changes of potential temperature and salinity make different contributions to density, with change of potential temperature being of more importance than that of salinity by a factor of ~ 2 at intermediate depths, NPIW loses its density to the south from a value of about 26.7 kg m^{-3} at 20°N to about 26.62 kg m^{-3} at 5°N (Fig. 11b). Here, the density of NPIW off Mindanao is somewhat higher than that derived from synoptic ob-

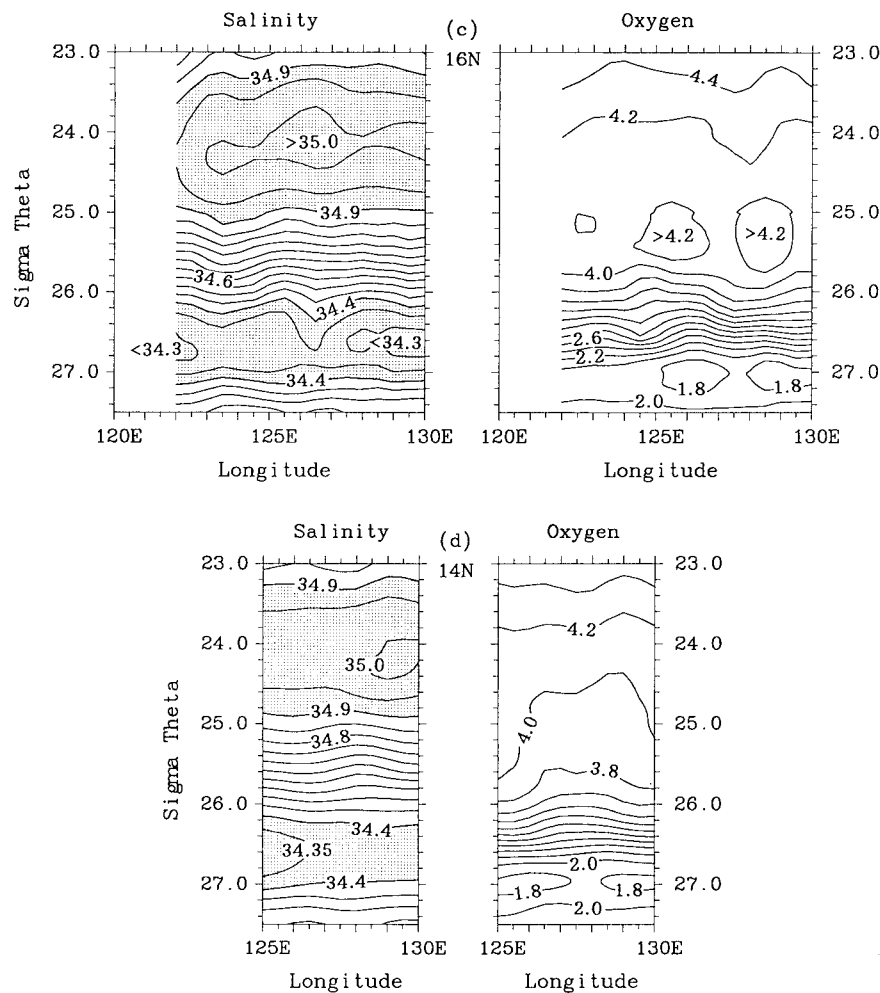


FIG. 9. (Continued.)

servations (Lukas et al. 1991; Bingham and Lukas 1994). This could be either due to the sparse vertical resolution of the data or due to the averaging and smoothing processes (described in section 4) used in preparing this mean density field.

Lukas et al. (1991) suggest that the lower NPIW density off Mindanao is due to truncation from below, as the deeper component of NPIW has been sheared off by the intrusion of AAIW. The effect of mixing, however, may also be important. Because of the different importance of potential temperature and salinity in the state equation, mixing of potential temperature and salinity are not jointly compensated. The net effect of mixing would be to change NPIW density in favor of potential temperature, that is, to decrease southward along the Philippine coast.

8. Discussion and summary

With all available historical and recent data, we have shown an updated climatology of the circulation and

water mass distribution near the Philippine coast. Though time variability and the possible errors in the data are rather large, the climatology has essentially the same pattern of circulation as that derived from synoptic measurements in the upper thermocline by several earlier studies, except for some quantitative differences; but, considerable discrepancies are found at intermediate depths mainly because of the poleward contraction of the subtropical gyre on denser surfaces.

The bifurcation of the NEC is measured near 20°N on the 27.2σ_θ surface, about 5° farther north than in the upper thermocline. The low part of the LUC does not appear to go directly southward along the western boundary, as is the case in the shallower waters. Perhaps, it separates from the coast at 10°–12°N and penetrates into the equatorial region through a clockwise recirculation east of Mindanao. There is some indication that this clockwise recirculation is mainly the Halmahera eddy, tilting to the northwest from about 3°N, 130°E near the surface to about 7°N, 127°E at intermediate depths. The mechanism responsible for the ex-

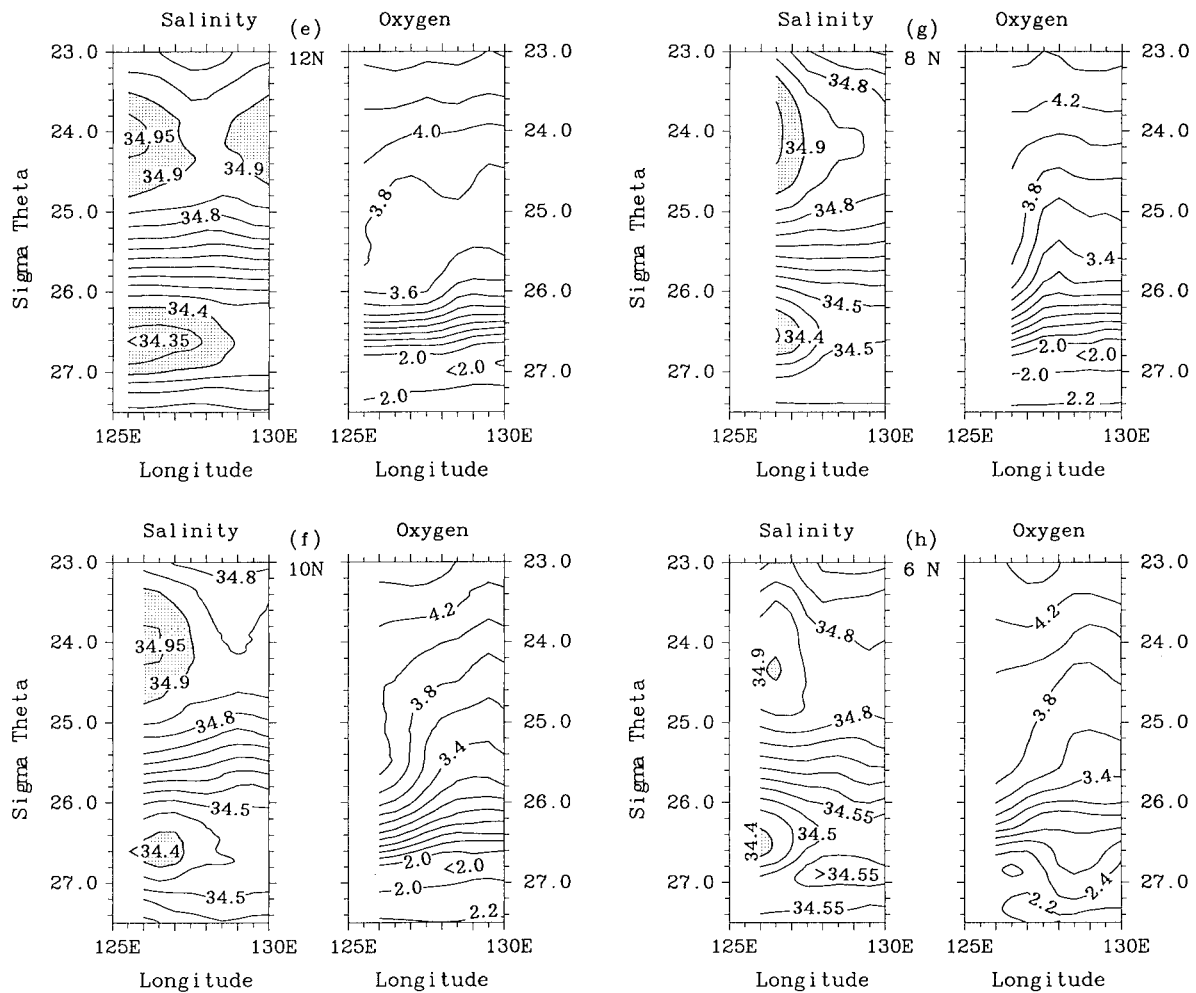


FIG. 9. (Continued.)

istence of this eddy may be a combination of thermohaline driving and topographic features (Masumoto and Yamagata 1991). Its shallow part does not expand northward probably because of the strong potential vorticity gradient associated with the southward turning of the NEC and its subsequent eastward flow of the NECC (Fine et al. 1994; Kashino et al. 1996). At increasing depths the NEC retreats northward and, in particular, to north of 15°N on density surfaces around $27.2\sigma_\theta$, producing negligible potential vorticity gradient off Mindanao (Kashino et al. 1996) and thus allowing the lower part of the Halmahera eddy to intrude farther northwest. As such, the previously observed northward-flowing MUC east of Mindanao appears to be merely a component of recirculation associated with the Halmahera eddy.

The Halmahera eddy may be a key factor concerning the water exchange between hemispheres. Especially at intermediate depths, this eddy extracts North Pacific water from the north and South Pacific water from the

south, and it finally allows the mixed water to flow southeastward into the equatorial circulation on its northeast side, westward to the Celebes Sea on its south side, and northward along the coast of Mindanao on its west side.

Consonant with the circulation pattern described above, NPTW and NPIW enter the western ocean with their extreme properties at about 15° and 20°N, respectively. Some of them continue southward as part of the LUC/MC. The southward intrusion of NPTW and NPIW is seen as far south as the southern tip of Mindanao along the western boundary. We found little evidence that SPTW flows into the Celebes Sea. Instead, much of this saline water appears to recurve eastward into the equatorial circulation through the shallow part of the Halmahera eddy, consonant with the hypothesis that the Indonesian Throughflow is largely derived from the MC waters (e.g., Lukas et al. 1991; Hautala et al. 1996). The influence of South Pacific sources becomes increasingly important with depth. On the $27.2\sigma_\theta$ surface, water

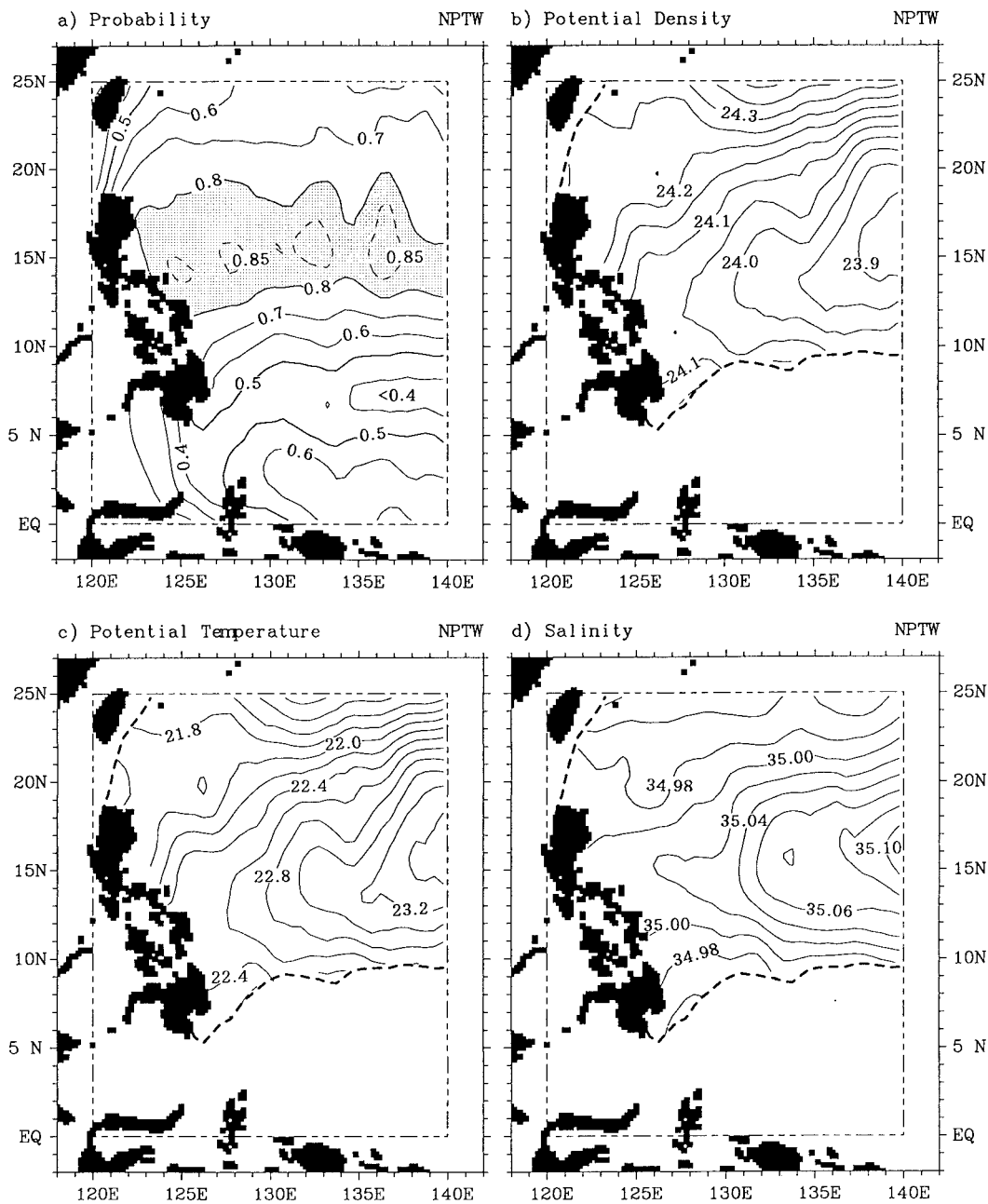


FIG. 10. Distributions of (a) probability, (b) potential density (in kg m^{-3}), (c) potential temperature (in $^{\circ}\text{C}$), and salinity (in psu) of NPTW, defined as a salinity maximum (>34.85 psu) in density range of $23.0\text{--}25.0\sigma_{\theta}$. The heavy dashed lines denote the 0.5 probability isopleth.

characteristic of AAIW is traced to about 12°N east of Mindanao; however, there is little indication of a northward flow of AAIW farther north as was expected (e.g., Reid 1965; Fine et al. 1994).

NPTW and NPIW are also traced as salinity extremes. Considerable changes in water properties are found at these salinity extremes because of mixing. Mixing of potential temperature and salinity, however, are not jointly compensated, thus leading to an increase of den-

sity in NPTW and a decrease of density in NPIW in their flowpath from the subtropical gyre to the Tropics with the NEC and the LUC/MC. These results suggest that whether or not a water mass remains a stable density should largely depend on the relative importance of potential temperature and salinity in the state equation.

Left to be addressed in future studies is the effect of eddies on the distribution of water masses. Although part of the standard deviation obtained during the av-

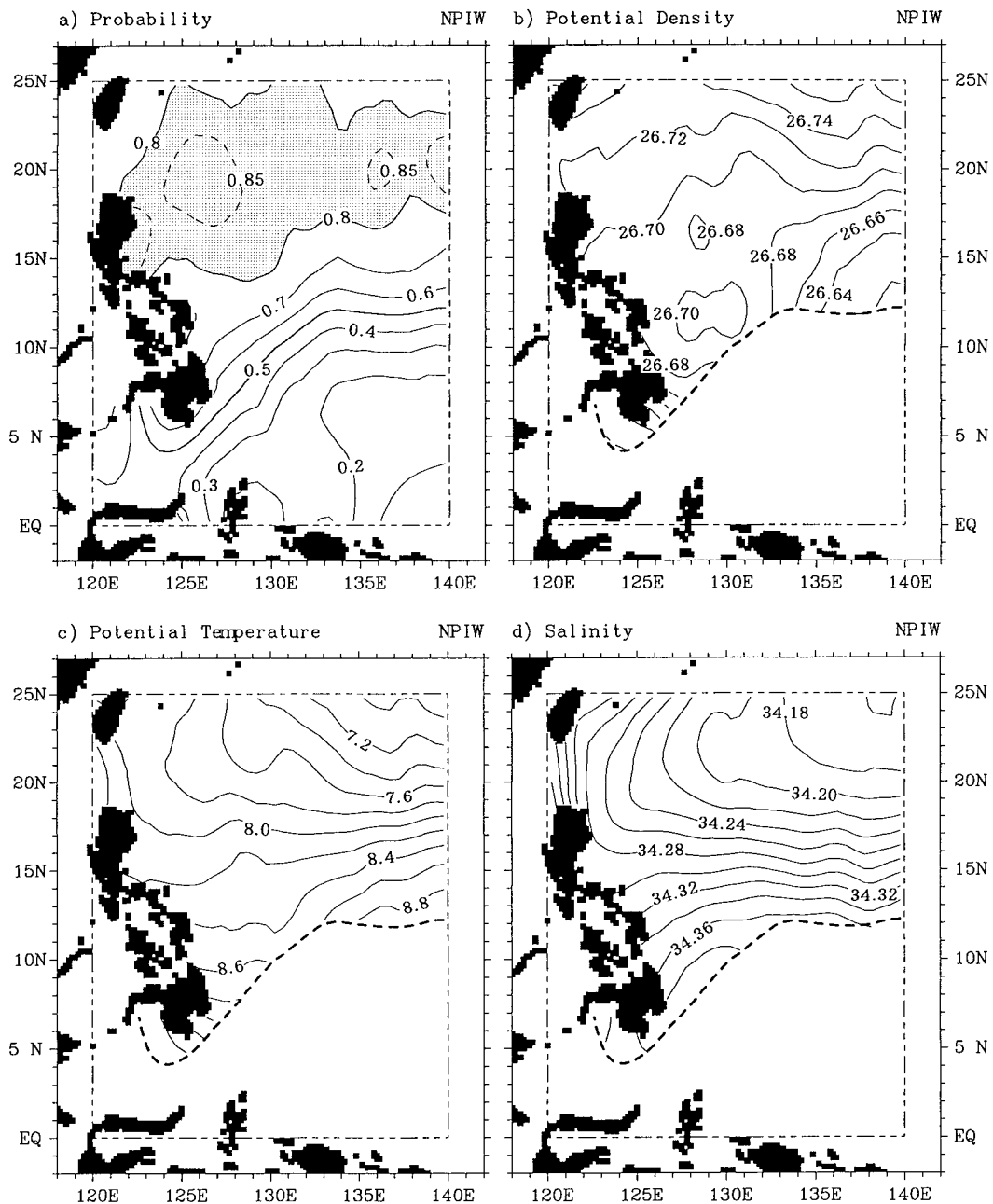


FIG. 11. Same as Fig. 10 except for NPIW, defined as a salinity minimum (<34.45 psu) in density range of $26.4\text{--}27.0\sigma_{\theta}$.

eraging process may be attributed to the limited number of samples and the sparse resolution of the data, time variability in the region appears to be of comparable strength with the mean field. In view of this large time variability, the combined use of data from various cruises in different seasons of different years may be justifiable for the flow due to the very large tendency for geostrophic balance in the horizontal momentum equations (Wijffels et al. 1995; Qu et al. 1998); but, the effect of eddies on the distribution of properties is not

likely to be filtered out by averaging, owing to the strong nonlinear dynamics in the process. In this regard, an eddy advective term representing the effect of baroclinic instability processes should be added to the mean advection. Whether the distribution of properties is more due to mean advection than due to eddy fluxes remains unknown. The limited observations available so far unfortunately do not permit a detailed investigation. Much work can be done with the emergence of high-resolution ocean general circulation models.

Finally, it is probably worthwhile noting that the poleward tilt of planetary eddies (e.g., the subtropical gyres, the Mindanao Dome, the Halmahera eddy, etc.) at increasing depth looks like a rather general phenomenon of the global ocean. The general dynamics governing this tilt should be investigated further by research.

Acknowledgments. The NODC data used for this study was kindly provided by the Japan Oceanographic Data Center; WOCE data by the WOCE Hydrographic Program—Special Analysis Center; CAS data by Institute of Oceanology, Chinese Academy of Sciences; PRC—USA data by State Oceanic Administration Data Center of China; JAMSTEC-BPPT data by Japan Marine Science and Technology Center; and WEPOCS III data by R. Lukas. We wish to express our deep thanks to N. Hogg for his constructive suggestions on the methods of objective analysis, and to G. Meyers, J. P. McCreary, R. Lukas, and S. Wijffels for their helpful discussions on the present topic. Thanks are also extended to J. Potemra and two anonymous reviewers for their valuable comments on the earlier manuscript. The International Pacific Research Center (IPRC) is partly sponsored by Frontier Research System for Global Change.

REFERENCES

- Bingham, F. M., and R. Lukas, 1994: The southward intrusion of North Pacific Intermediate Water along the Mindanao coast. *J. Phys. Oceanogr.*, **24**, 141–154.
- , and —, 1995: The distribution of intermediate water in the western equatorial Pacific during January–February 1986. *Deep-Sea Res. I*, **42**, 1545–1573.
- Bretherton, F. P., R. E. Davis, and C. B. Fandry, 1976: A technique for objective analysis and design of oceanographic experiments applied to MODE-73. *Deep-Sea Res. I*, **23**, 559–582.
- Fine, R. A., R. Lukas, F. M. Bingham, M. J. Warner, and R. H. Gammon, 1994: The western equatorial Pacific is a water mass crossroads. *J. Geophys. Res.*, **99**, 25 063–25 080.
- Gu, D., and S. G. H. Philander, 1997: Interdecadal climate fluctuations that depend on exchange between the Tropics and extratropics. *Science*, **275**, 805–807.
- Hautala, S. L., J. S. Reid, and N. Bray, 1996: The distribution and mixing of Pacific water masses in the Indonesian Seas. *J. Geophys. Res.*, **101**, 12 353–12 373.
- Hu, D., M. Cui, T. Qu, and Y. Li, 1991: A subsurface northward current off Mindanao identified by dynamic calculation. *Oceanography of Asian Marginal Seas*, K. Takano, Ed., No. 54, Elsevier Oceanogr. Series, Elsevier, 359–365.
- Kashino, Y., M. Aoyama, T. Kawano, N. Hendiarti, Syaefudin, Y. Anantasena, K. Muneyama, and H. Watanabe, 1996: The water masses between Mindanao and New Guinea. *J. Geophys. Res.*, **101**, 12 391–12 400.
- Levitus, S., and T. P. Boyer, 1994a: *World Ocean Atlas 1994*. Vol. 4: *Temperature*. NOAA Atlas NESDIS 4, U.S. Department of Commerce, 117 pp.
- , and —, 1994b: *World Ocean Atlas 1994*. Vol. 3: *Salinity*. NOAA Atlas NESDIS 3, U.S. Department of Commerce, 99 pp.
- , and —, 1994c: *World Ocean Atlas 1994*. Vol. 2: *Oxygen*. NOAA Atlas NESDIS 2, U.S. Department of Commerce, 186 pp.
- Lu, P., and J. P. McCreary, 1995: Influence of the ITCZ on the flow of thermocline water from the subtropical to the equatorial Pacific Ocean. *J. Phys. Oceanogr.*, **25**, 3076–3088.
- Lukas, R., E. Firing, P. Hacker, P. L. Richardson, C. A. Collins, R. Fine, and R. Gammon, 1991: Observations of the Mindanao Current during the Western Equatorial Pacific Ocean Circulation Study (WEPOCS). *J. Geophys. Res.*, **96**, 7098–7104.
- Luyten, J. R., J. Pedlosky, and H. Stommel, 1983: The ventilation thermocline. *J. Phys. Oceanogr.*, **13**, 292–309.
- Masumoto, Y., and T. Yamagata, 1991: Response of the western tropical Pacific to the Asian winter monsoon: The generation of the Mindanao Dome. *J. Phys. Oceanogr.*, **21**, 1386–1398.
- Masuzawa, J., 1972: Water characteristics of the North Pacific central region. *Kuroshio: Physical Aspects of the Japan Current*, H. Stommel and K. Yoshida, Eds., University of Washington Press, 95–127.
- McCreary, J. P., and P. Lu, 1994: On the interaction between the subtropical and the equatorial oceans: The subtropical cell. *J. Phys. Oceanogr.*, **24**, 466–497.
- Nitani, H., 1972: Beginning of the Kuroshio. *Kuroshio: Physical Aspects of the Japan Current*, H. Stommel and K. Yoshida, Eds., University of Washington Press, 129–163.
- Qiu, B., 1995: Why is the spreading of the North Pacific Intermediate Water confined on density surfaces around $\sigma_\theta = 26.8$? *J. Phys. Oceanogr.*, **25**, 168–180.
- , and R. Lukas, 1996: Seasonal and interannual variability of the North Equatorial Current, the Mindanao Current and the Kuroshio along the Pacific western boundary. *J. Geophys. Res.*, **101**, 12 315–12 330.
- Qu, T., T. Kagimoto, and T. Yamagata, 1997: A subsurface counter-current along the east coast of Luzon. *Deep-Sea Res. I*, **44**, 413–423.
- , H. Mitsudera, and T. Yamagata, 1998: On the western boundary currents in the Philippine Sea. *J. Geophys. Res.*, **103** (4), 7537–7548.
- Reid, J. L., 1965: Intermediate waters of the Pacific Ocean. *Johns Hopkins Oceanogr. Stud.*, Vol. 2, 85 pp.
- , and R. S. Arthur, 1975: Interpretation of maps of geopotential anomaly for the deep Pacific Ocean. *J. Mar. Res.*, **33** (Suppl.), 37–52.
- Talley, L. D., 1993: Distribution and formation of North Pacific Intermediate Water. *J. Phys. Oceanogr.*, **23**, 517–537.
- Toole, J. M., E. Zou, and R. C. Millard, 1988: On the circulation of the upper waters in the western equatorial Pacific Ocean. *Deep-Sea Res. I*, **35**, 1451–1482.
- , R. C. Millard, Z. Wang, and S. Pu, 1990: Observations of the Pacific North Equatorial Current bifurcation at the Philippine Coast. *J. Phys. Oceanogr.*, **20**, 307–318.
- Tsuchiya, M., 1968: Upper waters of the intertropical Pacific Ocean. *Johns Hopkins Oceanogr. Stud.*, Vol. 4, 50 pp.
- , R. Lukas, R. A. Fine, E. Firing, and E. Lindstrom, 1989: Source waters of the Pacific equatorial undercurrent. *Progress in Oceanography*, Vol. 23, Pergamon Press, 101–147.
- Wijffels, S., E. Firing, and J. Toole, 1995: The mean structure and variability of the Mindanao Current at 8°N. *J. Geophys. Res.*, **100**, 18 421–18 435.
- , M. M. Hall, T. Joyce, D. J. Torres, P. Hacker, and E. Firing, 1998: Multiple deep gyres of the western North Pacific: A WOCE section along 149°E. *J. Geophys. Res.*, **103**, 12 985–13 009.
- Wyrtki, K., 1961: Physical oceanography of the southeast Asian waters. NAGA Report 2, Scripps Inst. of Oceanogr., University of California, San Diego, La Jolla, CA, 195 pp.